Determination of 2D Directional Field of Three-point Bending Beam with Three-stepped Data in Digital Photoelasticity

Pichet Pinit
Department of Mechanical Technology Education
King Mongkut's University of Technology Thonburi
126 Pracha-uthit Rd., Bangmod, Tungkru, Bangkok 10140, Thailand
E-mail: pichet.pin@kmutt.ac.th

Eisaku Umezaki
Department of Mechanical Engineering
Nippon Institute of Technology
4-1 Gakuendai, Miyashiro, Saitama 345-8501, Japan

Abstract

This paper is to present a three-step color phase shifting approach for automatic determination of the directional field of stresses based on the results of a digitally photoelastic experiment. A plane polariscope with a white light source is used for recording the necessarily photoelastic fringe patterns. Relevant theories of the irradiance equations based on the use of the plane polariscope are derived. The obtained wrapped range of the isoclinic parameter is unwrapped to get the physical range by the unwrapping process. The obtained results in the physical range are compared to those obtained from the four-step phase shifting technique. The unwrapped results show that the method proposed herein provides reasonable accuracy.

Keywords: color phase shifting, directional field, digital photoelasticity, phase unwrapping, three-point bending beam

1. Introduction

Photoelasticity is an optical-experimental interference technique used for analyzing the stress induced in transparent models (birefringent models) due to applied loads. The principle of photoelasticity is based on the phenomenon of double refraction. This phenomenon can be clearly observed by looking through the optical element called a polariscope. The results interpreted from photoelasticity can be directly applied to prototypes or metals by using the law of similarity, provided that, the geometry of the prototypes and the transparent models are similar and the applied loads are also the same for both [1].

Photoelasticity provides two interference fringe patterns, i.e., an isoclinic fringe pattern and an isochromatic fringe pattern. These fringe patterns are used to extract two field parameters: an isoclinic parameter ϕ and an isochromatic parameter δ. They relate to the principal-stress direc-

tions and the principal-stress differences $(\sigma_1 - \sigma_2)$, respectively.

In case of ϕ, several researchers [2-7] proposed techniques to determine it. However, they often encounter two important problems: an effect of δ on ϕ [1] and a wrapped range of ϕ. The first problem occurs because the two fringe patterns are completely mixed known as photoelastic fringe pattern.

The second problem exists because a physical range of ϕ, i.e., $(-\pi/2, +\pi/2]$ where $(a, b]$ means $a < \phi \leq b$, is always larger than that obtained from calculation. This is because there always is a reduction factor that reduces the physical range to smaller ones.

To solve the second problem, phase unwrapping (PU) is needed. PU is the process of recovering the physical range of ϕ from its wrapped ones. Knowing ϕ in its physical range simply enables the stress components σ_{xx}, σ_{yy}, and τ_{xy} to be determined.

The main limitation of those techniques [2-7] is that they cannot be applied to a problem having discontinuities in the fringe field of the isoclinics. These discontinuities are the results of singularities [8]. Although some techniques [2,3] can, in principle, deal with the discontinuities, the range of ϕ obtained are of either $[0, +\pi/2]$ or $(-\pi/4, +\pi/4]$ with modulo $+\pi/2$ which still is of the wrapped range.

Recently, the present authors have proposed a method to automatically solve those two important problems [9]. In that work, the four-step phase shifting technique was used to determine ϕ and the developed PU algorithm can cope with the problem of the discontinuities. The obtained results of ϕ are reliable and of the physical range $(-\pi/2, +\pi/2]$; however, the technique needs four photoelastic fringe patterns.

To effectively determine the photoelastic parameters (ϕ and δ), a newly developed technique should contain the following aspects [1].

1. Accounting for the background irradiance.
2. Suitability to determine both ϕ and δ
3. Ease for PU of fractional fringe order or retardation
4. Capability to generate continuous map of ϕ representing only one of the principal stress directions (σ_1 or σ_2)
5. Accuracy of the evaluated parameters
6. The total number of fringe images needed

Based on the fourth, fifth, and sixth aspects, the present authors have proposed a three-step phase shifting technique to unwrap the isoclinic parameter [10]. However, only the circular disk under the vertically diametral compression was considered. It is well known that this model contains no isotropic points in the fringe field.

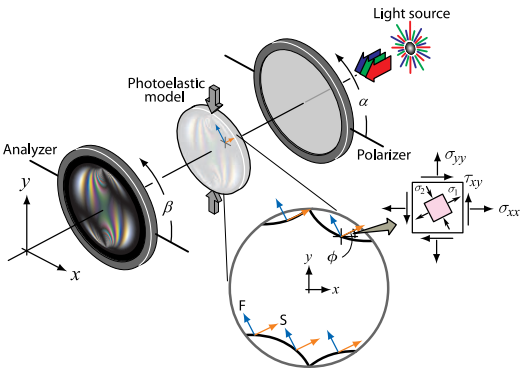

Fig. 1 Generic orientation of the plane polariscope. α, β, and ϕ are the angles of the polarizing axis of the polarizer, the polarizing axis of the analyzer, and the σ_1 direction with respect to the reference axis (x-axis), respectively. F and S respectively denote the fast and slow polarizing axes of the model.

This paper, then, presents a technique to determine ϕ using the three-step phase-shifting technique. The problem of a simply supported rectangular beam carrying a concentrated load at the center, which contains the isotropic points in the fringe field, is used for the evaluation.

2. Determination of Isoclinic Parameter ϕ

2.1 Dark-field Irradiance Equation

Consider the generic plane polariscope with a white light source (Figure 1) [9]. When the specimen is properly placed in the system and, then, loaded, the general equation of the irradiance I with generic orientations of the transmission axes of the polarizer and analyzer in a crossed fashion ($\alpha = \beta + \pi/2$) coming out of the analyzer is given by [1]:

$$I_{m,\lambda} = I_{\text{mod},\lambda} \sin^2 2(\phi - \beta_m) + I_{\text{b}} \tag{1}$$

where

$$I_{\text{mod},\lambda} = \frac{1}{\Delta\lambda} \int_{\lambda_1}^{\lambda_2} I_{\text{p},\lambda} \sin^2(\pi N_\lambda)\, d\lambda \tag{2}$$

In Equation (1) and (2), m is the step number of the angular positions of the crossed polarizer and analyzer, $\lambda(= R, G, B)$ is the primary wavelengths of the white light source, $\Delta\lambda$ is the difference between the upper limit wavelength, λ_2, and the lower limit wavelength, λ_1, of the light spectrum, $I_{\text{mod},\lambda}$ is the modulated irradiance, $I_{\text{p},\lambda}$ is the irradiance coming out of the polarizer, N_λ is the fractional fringe order for a given wavelength of the light source used, ϕ is the isoclinic parameter or the angle of σ_1 with respect to the reference axis, β_m is the phase shift angle at the step m, $I_{\text{b}}$is the total background irradiance for the entire spectrum.

Table 1 Plane polariscope arrangement and irradiance equations for three steps of the intermediate phase-shifted angle ω

m	ω	Irradiance equation
1	$-\theta$	$I_{1,\lambda} = I_{\text{eff},\lambda} - \frac{1}{2} I_{\text{mod},\lambda} \sin(\eta - \theta)$
2	0	$I_{2,\lambda} = I_{\text{eff},\lambda} - \frac{1}{2} I_{\text{mod},\lambda} \sin(\eta)$
3	$+\theta$	$I_{3,\lambda} = I_{\text{eff},\lambda} - \frac{1}{2} I_{\text{mod},\lambda} \sin(\eta + \theta)$

The relation between the fractional retardation and the fractional fringe order can be expressed as:

$$\delta_\lambda = 2\pi N_\lambda \tag{3}$$

For simplicity, Equation (1) may be rewritten as:

$$I_{m,\lambda} = I_{\text{eff},\lambda} - \tfrac{1}{2} I_{\text{mod},\lambda} \sin(\eta + \omega_m) \tag{4}$$

where

$$I_{\text{eff},\lambda} = \tfrac{1}{2} I_{\text{mod},\lambda} + I_{\text{b}} \tag{5a}$$

$$\eta = \tfrac{1}{2}\pi - 4\phi \tag{5b}$$

$$\omega_m = 4\beta_m \tag{5c}$$

Equations (5a) and (5c) are respectively termed as the effective background irradiance and the virtual or intermediate phase-shifted angle. Furthermore, the angle β (the angle between the polarizing axis of the analyzer and the reference axis) can be only in the range of $[0, +\pi/2]$.

2.2 Computation of Isoclinic Parameter

Applying three steps of the intermediate phase-shifted angle so that:

$$\omega_m = \{\theta(m-2) \mid m = 1, 2, 3\} \tag{6}$$

and, then, substituting ω_m into Equation (4), yield three irradiance equations for three steps. Table 1 lists these irradiance equa-

tions. Combining these three equations by setting $\theta = +4\pi/6$ [10], the expression used for determination of ϕ can be obtained as:

$$\phi_{\text{wr}} = \frac{\pi}{8} - \frac{1}{4}\arctan\left\{\frac{I_1^{\text{s}} + I_3^{\text{s}} - 2I_2^{\text{s}}}{\sqrt{3}\left(I_1^{\text{s}} - I_3^{\text{s}}\right)}\right\} = \frac{\pi}{8} - \frac{1}{4}\arctan\left(\frac{I_{\text{sin}}}{I_{\text{cos}}}\right) \quad (7)$$

where

$$I_m^{\text{s}} = I_{m,\text{R}} + I_{m,\text{G}} + I_{m,\text{B}} \quad (8a)$$

$$I_{\text{sin}} = I_1^{\text{s}} + I_3^{\text{s}} - 2I_2^{\text{s}} \quad (8b)$$

$$I_{\text{cos}} = \sqrt{3}\left(I_1^{\text{s}} - I_3^{\text{s}}\right) \quad (8c)$$

and

$$I_{\text{mod}}^{\text{s}} = \sqrt{\tfrac{4}{3}[(I_1^{\text{s}} - I_3^{\text{s}})^2 + \tfrac{1}{3}(I_1^{\text{s}} + I_3^{\text{s}} - 2I_2^{\text{s}})^2]} \quad (9a)$$

$$I_{\text{eff}}^{\text{s}} = I_{\text{eff,R}} + I_{\text{eff,G}} + I_{\text{eff,B}} \quad (9b)$$

The subscript 'wr' in Equation (7) denotes that the computed values of ϕ are of the wrapped range and $\phi_{\text{wr}} \in [0, +\pi/4]$ due to the use of the ordinary inverse tangent function.

It is worthy to mention that before substituting the results obtained from Equation (8a) into Equation (7), the irradiance summation should be normalized by a factor such that the summation does not exceed the maximum gray level used in the calculation [7,9]. Furthermore, although Equation (7) is derived from the three-stepped phase shift on the basis of the use of Equation (4) with a white light source, Equation (7) is still valid and this is due to the fact that the use of a white light source modifies only the isochromatic fringe pattern but not the isoclinic one (see Equation (1) and the meaning of $I_{\text{mod},\lambda}$ in Equation (2)).

It is also important to note that Equation (7) is mathematically indeterminate when $I_{\text{mod}}^{\text{s}} = 0$ and this is well known s the isochromatic-isoclinic interaction. This interaction causes errors in the isoclinic map. However, in practical, the errors also occur when the values of $I_{\text{mod}}^{\text{s}}$ are close to zero.

Table 2 Conditions used for transforming the range of $[0, +\pi/4]$ to $[0, +\pi/2]$

Condition	$\phi_{\text{wr}} \in [0, +\pi/2]$
$I_{\text{cos}} < 0$	$\phi_{\text{wr}} = \text{Eq. (7)} + \pi/4$
$I_{\text{sin}} > 0$ and $I_{\text{cos}} = 0$	$\phi_{\text{wr}} = +\pi/2$
$I_{\text{sin}} < 0$ and $I_{\text{cos}} = 0$	$\phi_{\text{wr}} = +\pi/4$
else	Eq. (7)

Table 3 Conditions used for transforming the range of $[0, +\pi/4]$ to $(-\pi/4, +\pi/4]$

Condition	$\phi_{\text{wr}} \in (-\pi/4, +\pi/4]$
$I_{\text{cos}} < 0$	$\phi_{\text{wr}} = \text{Eq. (7)} - \pi/4$
$I_{\text{sin}} > 0$ and $I_{\text{cos}} = 0$	$\phi_{\text{wr}} = +\pi/4$
$I_{\text{sin}} < 0$ and $I_{\text{cos}} = 0$	$\phi_{\text{wr}} = 0$
else	Eq. (7)

3. Unwrapping of Isoclinic Parameter [9]

The PU algorithm used for determining the unwrapped directional field or the isoclinics in the physical range ϕ_{pr} is the same as that already proposed [9]. For the sake of clarity, it is briefly described here. It should be noted that the subscript 'pr' denotes that ϕ is in the physical range of $(-\pi/2, +\pi/2]$.

The whole unwrapping process can be systematically divided into three states: (1) preprocessing, (2) main processing, and (3) post processing. They are briefly explained as follows:

Preprocessing

(1) Calculate ϕ_{wr} using Equation (7).

(2) Extend the calculated ϕ_{wr} to the ranges of $[0, +\pi/2]$ and $(-\pi/4, +\pi/4]$ using simple logic operations shown in Tables 2 and 3, respectively. Each of these two ranges is recorded as an image or map.

(3) Identify the valid regions. To record the valid regions, create a binary array and initially populates it with 0 values. These regions can be determined by performing a raster scan over the map of range of $(-\pi/4, +\pi/4]$. When scanning, for any pixel whose isoclinic value is in the range of $(-\pi/8, +\pi/8]$, that pixel in the binary array is set to 1.

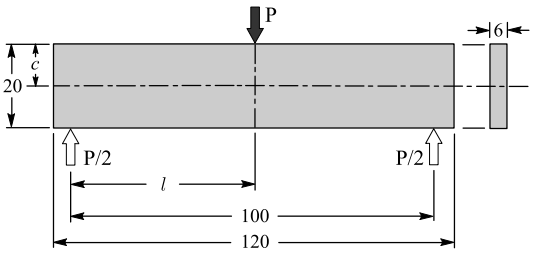

Fig. 2 Geometrical shape and the direction of the applied load (black arrow) and supports (white arrows) of the three-point bending beam (P = 314 N, $l = 50$ mm and $c = 10$ mm) [9].

(4) Detect the singularities using the double function [8]. Then, expand areas around the singularities and exclude them from the valid regions in the binary array in step 3.

(5) Detect the largest region in the binary array using the connected component labeling. This algorithm assigns different integer numbers for different regions of white pixels. The assigned number having the largest region is selected. The left pixels are set to 0.

(6) Create an array of floating point values for keeping the final results of ϕ_{pr}. Transfer the isoclinic of the range of $(-\pi/4, +\pi/4]$ to the created array using the largest region detected in step 5 as a filter. That is, for white pixels in the binary array, the values of isoclinics can be transferred.

Main processing

(7) Scan to find pixels lying on the boundary of the largest region in the binary array. These pixels are recorded into an adjoin array (one-dimensional array) in ascending order of the absolute difference between the isoclinic values of those pixels found in the array and their mean; that is, the first element of the array keeps the pixel having the smallest absolute difference and the last element records the largest absolute difference.

(8) Each time, the element of the adjoin array is accessed orderly from the first element and this element is used to be a central pixel of a 3×3 unwrapping box. The wrapped pixels locating inside this box are then unwrapped, comparing to the central pixel. The way to unwrap is similar to that described [9] and it is not described here. The process continues until all of wrapped pixels in the region of interest are completely visited and unwrapped.

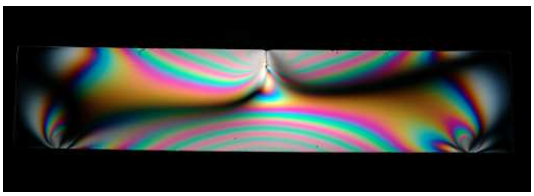

(a)

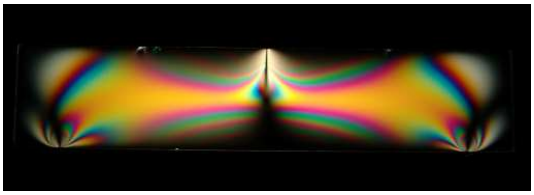

(b)

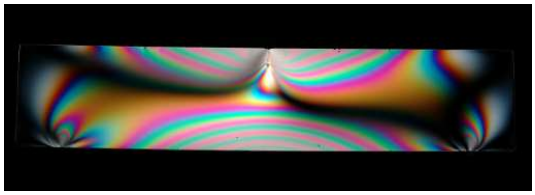

(c)

Fig. 3 550 × 200-pixels color photoelastic fringe images of the three-point bending beam, experimentally recorded at: (a) $\beta_1 = -\pi/6$. (b) $\beta_2 = 0$. (c) $\beta_3 = +\pi/6$. (Printed in black and white)

Post processing

This final process performs mapping ϕ_{pr} to gray level to ease visualization. The gray level used is 256 steps where 0 represents pitch black and 255 represents pure white. The unwrapped values of ϕ_{pr} in the range of $(-\pi/2, +\pi/2]$ are, then, linearly mapped into the gray level range of [0, 255].

4. Experimental Setup and Results

Figure 1 shows the schematic of the plane polariscope used for capturing the photoelastic fringe images. The polariscope mainly consists of a light source, polarizer, photoelastic model, and analyzer. The photoelastic fringe images were recorded with a digital camera. The photoelastic model used here is the three-point bending beam and it was made of an epoxy resin plate. Figure 2 shows the geometry and loading conditions [9].

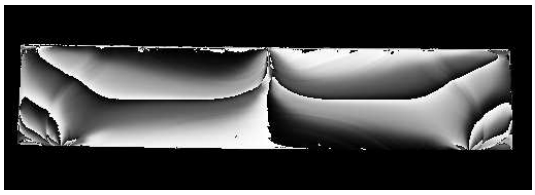

(a)

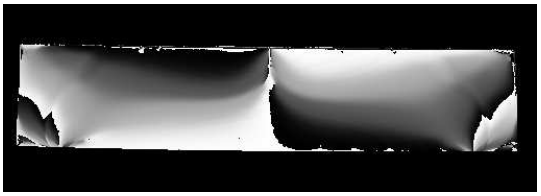

(b)

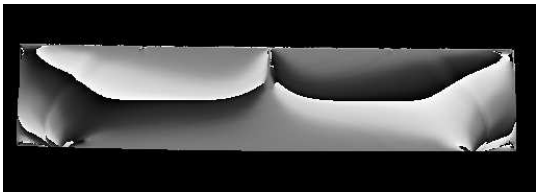

(c)

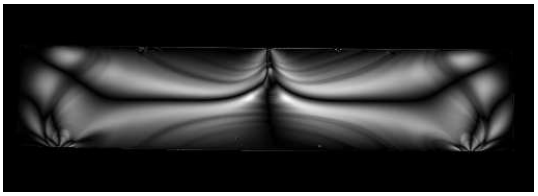

(d)

Fig. 4 Numerically generated maps: (a) wrapped isoclinics in the range of $[0, +\pi/4]$. (b) wrapped isoclinics in the range of $[0, +\pi/2]$. (c) wrapped isoclinics in the range of $(-\pi/4, +\pi/4]$. (d) normalized modulated irradiance in the range of [0, 1]. The values of each range are separately codified by the gray scale range of [0, 255] where 0 represents deep black and 255 represents pure white.

Figure 3 shows the photoelastic fringe images recorded by the plane polariscope (Figure 1) with different angular position of angle β. In these images, the isoclinic fringe and isochromatic fringe are completely mixed. The use of Equation (7) is to separate these fringe images with the condition $I^{s}_{\text{mod}} \neq 0$. Figure 4 displays the generated maps of wrapped isoclinics and modulated irradiance.

(a)

(b)

(c)

Fig. 5 Maps of binary images and the first region: (a) valid region. (b) largest region. (c) first region.

Figure 4a was obtained from the use of Equation (7) with the photoelastic images (Figure 3), whereas Figures 4b and 4c were given from Figure 4a with the simple logic operations shown in Tables 2 and 3, respectively. Figure 5 shows the binary image representing the valid regions, the largest region and the first region. The valid regions (Figure 5a) were obtained from step 3 and the largest region (Figure 5b) was given from step 5. The first region (Figure 5c) was generated at step 6. The black regions in Figure 5a occurred when the condition mentioned in step 3 was not satisfied.

Figure 6 displays the maps of unwrapped isoclinics obtained from the three-stepped method and the four-stepped method [10]. Figure 7 shows the profiles of the isoclinic values along the dashed line shown in Figure 6a, whereas Figure 8 shows the plot of the difference of those profiles.

5. Discussion

It is seen in Figures 3 and 4d that the left and right sharp edges of the beam are subjected to small amounts of stresses; that is, at these regions, the photoelastic fringe images appeared as black color (almost black). These regions refer to the zeroth fringe order ($N = 0$).

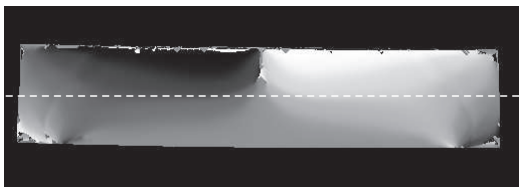

(a)

(b)

Fig. 6 Map of unwrapped isoclinics in the range of $(-\pi/2, +\pi/2]$: (a) map obtained from the three-step method proposed here and (b) map obtained from the four-step method [10]. Black represents $-\pi/2$ and white represents $+\pi/2$.

One can see, in Figure 4d, the dark line which coincides with the neutral axis of the beam as in the case of the four-point bending beam. However, the line does not represent the natural axis but it is actually the isoclinic of any parameter. Therefore, the stress difference $(\sigma_1 - \sigma_2)$ is not zero along this line.

This problem contains two isotropic points [11] near each other and they can be observed as a circle-like region near the middle part of the beam (Figure 4b). The upper isotropic point is of negative type, whereas the lower one is of positive type [11]; however, they are vague. This vague-

ness makes the stress trajectories more complex around such a region.

Figure 5a was given by scanning over Figure 4c with the condition mentioned in step 3. After masking out the positions of the singularities [8] and applying the connected component labeling algorithm, the largest region was selected as shown in Figure 5b. Figure 5c was given by transferring the isoclinic values as mentioned in step 6 and this is the first region used to start the phase unwrapping process.

Upon completing the unwrapping process, the map of unwrapped isoclinics was given and it is shown in Figure 6a. The map of unwrapped isoclinics obtained by the four-stepped method is displayed in Figure 5b.

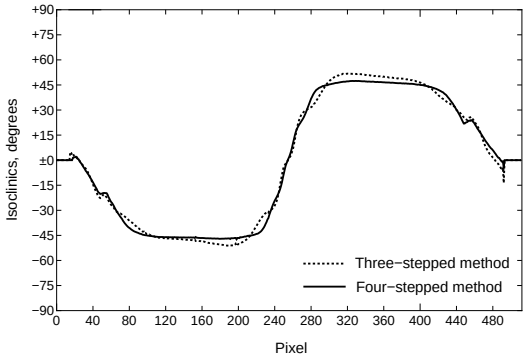

Fig. 7 Comparison of profiles of isoclinic values along the dashed line drawn over Figure 6a. The dotted line and solid line are respectively of Figures 6a and 6b.

One can see that these maps are almost similar. Their difference is at the upper layer of the beam. This difference might be the contribution of the residual stress occurred due to the preparation of the model.

The profiles of the isoclinic values along the dashed line drawn over Figure 6a, obtained from both three- and four-stepped methods, are shown in Figure 7. It is seen that they agree well; however, they are different for the portions between the point of the applied load and the supports. Figure 8 shows the difference of the isoclinic values obtained between both methods. It is seen that the absolute difference is about 8 degrees at the 230th pixel number, which is near the position of the isotropic points. As a consequence, this largest difference might be the effect of such isotropic points, since at them, the isoclinics are indeterminate.

6. Conclusion

A three-stepped method was proposed for determining the isoclinic parameter in its physical range of $(-\pi/2, +\pi/2]$. The method was verified with a three-point bending beam having isotropic points. Based on the recommended aspects previously mentioned, the three-stepped method provided reasonable accuracy of isoclinics compared with those obtained from the four-stepped method.

Since the map of unwrapped isoclinics now represents only one of the principal stress directions (σ_1), it can be used in the stress separation process for individually determining the principal stresses.

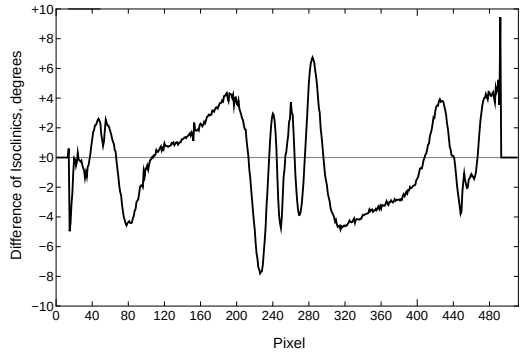

Fig. 8 Difference of isoclinic values obtained between the four-stepped method and the three-stepped method.

7. References

[1] Ramesh, K., Digital Photoelasticity: Advanced Technique and Applications, Springer, Berlin, 2000.

[2] Patterson, E.A. and Wang, Z.F.,

Towards Full Field Automated Photoelastic Analysis of Complex Components, Strain, Vol. 27, No. 2, pp. 49-56, 1991.

[3] Buckberry, C. and Tower, D., New Approaches to the Full-field Analysis of Photoelastic Stress Patterns, Opt. Lasers Eng., Vol. 24, No. 5-6, pp. 415-428, 1996.

[4] Nurse, A.D., Full-field Automated Photoelasticity by Use of a Three-wavelength Approach to Phase Stepping, Appl. Opt., Vol. 36, No. 23, pp. 5781-5786, 1997.

[5] Plouzennec, N. and Lagarde, A., Two-wavelength Method for Full-field Automated Photoelasticity, Exp. Mech., Vol. 39, No. 4, pp. 274-277, 1999.

[6] Kihara, T., An Arctangent Unwrapping Technique of Photoelasticity Using Linearly Polarized Light at Three Wavelengths, Strain, Vol. 39, No. 2, pp. 65-71, 2003.

[7] Pinit, P. and Umezaki, E., Full-field Determination of Principal-stress Directions Using Photoelasticity with Plane Polarized RGB Lights, Opt. Rev., Vol. 12, No. 3, pp. 228-232, 2005.

[8] Pinit, P., Automated Detection of Singularities from Orientation Map of Isoclinics in Digital Photoelasticity, Proceeding of the 21st Conference of Mechanical Engineering Network of Thailand, Chonburi, Thailand, pp. 1-10, 2007.

[9] Pinit, P. and Umezaki, E., Digitally Whole-field Analysis of Isoclinic Parameter in Photoelasticity by Four-step Color Phase-shifting Technique, Opt. Lasers Eng., Vol. 45, No. 7, pp. 795-807, 2007.

[10] Pinit, P., Susumu, T., and Umezaki, E., Determination of Principal-stress Directions by Three-step Color Phase Shifting Technique, Key Eng. Materials, Vol. 321-323, pp. 1284-1287, 2006.

[11] Frocht, M.M., Photoelasticity, Vol. II, John Willey & Sons, New York, 1948.